

Identification of a Residue Involved in Transition-State Stabilization in the ATPase Reaction of DNA Gyrase[†]

Clare V. Smith and Anthony Maxwell*

Department of Biochemistry, University of Leicester, University Road, Leicester LE1 7RH, U.K.

Received January 20, 1998; Revised Manuscript Received April 30, 1998

ABSTRACT: Examination of the X-ray crystal structure of the 43 kDa N-terminal domain of the DNA gyrase B protein (GyrB) shows that the majority of the interactions with bound ATP are made with subdomain 1 (residues 2–220). However, two residues from subdomain 2, Gln335 and Lys337, interact with the γ -phosphate of ATP. The proposed roles for these residues include nucleotide binding, transition-state stabilization, and triggering protein conformational changes. We have used site-directed mutagenesis to convert Gln335 to Asn and Ala and Lys337 to Gln and Ala in the N-terminal domain of GyrB. Two of the resultant mutant proteins, GyrB43^{Q335A} and GyrB43^{K337Q}, were shown to be correctly folded, and their interactions with ATP have been analyzed in detail. The Q335A protein is apparently unchanged with regard to nucleotide binding and hydrolysis, whereas the K337Q protein shows a modest decrease in nucleotide binding and a drastic reduction in ATPase activity. This is manifested by a $\sim 10^3$ -fold decrease in k_{cat} . When the two mutations were moved into full-length GyrB, the Q335A mutation again showed little or no effect on activity, whereas the K337Q mutation had undetectable supercoiling and ATPase activities. We conclude that Gln335 is dispensable for ATP binding and hydrolysis by the gyrase B protein, whereas Lys337 has a critical role in the ATPase reaction and is likely to be a key residue in transition-state stabilization.

DNA gyrase is a bacterial type II topoisomerase which catalyzes the energetically unfavorable negative supercoiling of DNA by coupling this reaction to the hydrolysis of ATP (1, 2). While all topoisomerases are able to relax negatively supercoiled DNA, gyrase is unique in its supercoiling activity. The enzyme from *Escherichia coli* consists of two proteins (A and B) with molecular masses of 97 and 90 kDa, respectively. The active enzyme is an A₂B₂ complex. In addition to DNA supercoiling, gyrase can also catalyze the relaxation of both positively and negatively supercoiled DNA, the knotting and unknotting of DNA and the catenation and decatenation of duplex circles.

The mechanism of DNA supercoiling by gyrase involves the following steps: (i) wrapping a segment of DNA (~ 130 bp) around the enzyme in a positive superhelical sense; (ii) cleavage of the wrapped DNA in both strands with the formation of covalent bonds between the newly formed 5'-phosphates and Tyr122 of the A subunits; (iii) passage of another segment of the broken DNA through this double-stranded break; and (iv) resealing of the broken DNA, leading to a reduction in the linking number of 2 (i.e., the introduction of two negative supercoils). The driving force for this energetically unfavorable reaction comes from ATP hydrolysis; it is thought that two molecules of ATP are hydrolyzed per supercoiling cycle. The mechanism of energy coupling between ATP hydrolysis and DNA supercoiling is not fully understood. When a nonhydrolyzable ATP analogue, AD-PNP¹ (5'-adenylyl β , γ -imidodiphosphate), binds to gyrase,

limited supercoiling is seen. This suggests that the conformational changes associated with nucleotide binding can induce one supercoiling event, but catalytic supercoiling requires the hydrolysis of ATP and dissociation of products (1–3).

A number of lines of evidence demonstrate that the GyrA and GyrB proteins contain distinct functional domains. GyrA consists of a N-terminal domain (59–64 kDa); the structure of a 59 kDa N-terminal fragment has recently been determined to 2.8 Å by X-ray crystallography (4). This domain is involved in DNA breakage and reunion, while the C-terminal 33 kDa domain is involved in DNA wrapping (5–7). The B protein also consists of two domains. The N-terminal 43 kDa domain (GyrB43) contains the ATP-binding site and has been shown to hydrolyze ATP. The structure of this domain complexed with ADPNP has been solved to 2.5 Å resolution by X-ray crystallography (8). The C-terminal 47 kDa domain interacts with A protein and DNA (9–12).

Gyrase is the target of a number of antibacterial agents, many of which belong to one of two groups: the quinolones and the coumarins (for a review, see ref 13). Quinolone drugs (e.g., oxolinic acid and ciprofloxacin) inhibit DNA supercoiling by interrupting the breakage and reunion of DNA by gyrase. The coumarin drugs (e.g., novobiocin and chlorobiocin) inhibit supercoiling by preventing the hydroly-

[†] This work was funded by the Wellcome Trust. C.V.S. was supported by a Wellcome Prize studentship. A.M. is a Lister-Institute Jenner Fellow.

* Corresponding author.

¹ ADPNP, 5'-adenylyl- β , γ -imidodiphosphate; CD, circular dichroism; DHN, dihydronovobiocin; DMS, dimethyl sulfoxide; DTT, dithiothreitol; GyrA, DNA gyrase A protein; GyrB, DNA gyrase B protein; GyrB43, N-terminal 43 kDa domain of GyrB; IPTG, isopropyl β -D-thiogalactopyranoside; PK/LDH, pyruvate kinase and lactate dehydrogenase; ts, temperature sensitive.

sis of ATP by gyrase (14). The binding site for coumarins has been shown to be in the 43 kDa N-terminal domain of GyrB; mutations conferring resistance have been found in this domain (15, 16). The structure of an N-terminal subdomain of GyrB (24 kDa; residues 2–220) complexed with novobiocin has recently been determined (17), as well as the complex of this subdomain with chlorobiocin (18). These data, together with recent binding data (19), support the idea that these drugs are competitive inhibitors of ATP hydrolysis, with the binding sites of ATP and novobiocin partially overlapping.

ATP hydrolysis by GyrB43 shows distinctly non-Michaelis–Menten kinetics (12). The greater than first-order dependence of rates on enzyme concentration suggests that the active form of the enzyme is an oligomer. This has also been observed in the case of GyrB alone (20, 21). The kinetic data are consistent with a scheme in which the active enzyme is a dimer. This is supported by the X-ray crystal structure of this domain, which shows that the protein is a dimer in the presence of ADPNP (8). Protein cross-linking studies (22), gel filtration, and ultracentrifugation (12) also indicate dimers in the presence of ADPNP, but not in its absence.

A scheme for the hydrolysis of ATP has been proposed in which ATP can bind to the 43 kDa monomer, but the protein is only active upon dimerization (12). This dimeric complex hydrolyzes ATP leading to product release and dissociation into the monomeric form. Dimerization is found to be rate limiting and it is assumed that the hydrolysis step is rapid. A steady-state rate equation, consistent with this scheme, has been derived (12). ADPNP binding to this domain has also been studied, and the data are consistent with a scheme in which the 43 kDa monomer forms a short-lived complex with ADPNP that can be converted into a long-lived dimer complex containing either 1 or 2 molecules of bound ADPNP; dimer formation with two bound ADPNPs is strongly favored (22).

The X-ray crystal structure of the N-terminal GyrB has allowed a close examination of the residues involved in nucleotide binding and those potentially involved in hydrolysis. A mechanism for hydrolysis has been proposed in which Glu42 of GyrB acts as a general base and His38 has a role in aligning and polarizing the glutamate residue; this mechanism is supported by site-directed mutagenesis experiments (23). Lys103, initially identified by specific labeling of GyrB using the ATP-affinity analogue pyridoxal 5'-diphospho-5'-adenosine (PLP-AMP) (24), has been investigated, and its role in ATP binding has been established by site-directed mutagenesis (25). The crystal structure shows that this residue forms a salt bridge with the β -phosphate of ADPNP (Figure 1, top panel). Other residues which can be seen to contribute to the ATP-binding site include Tyr109 and Asp73, which make polar contacts with the adenine ring of ADPNP, and Tyr5 from the N-terminal arm of the other molecule of the dimer contacts the 5'-hydroxyl group of the ribose ring. These residues all lie in subdomain 1 (residues 2–220) of GyrB43. Figure 1, top panel, shows hydrogen-bonding contacts to the β - and γ -phosphates. The residues shown are almost exclusively in subdomain 1, however, there are two residues which lie in subdomain 2 (residues 221–393) which are also within hydrogen-bonding distance of the γ -phosphate of the ADPNP; these are Gln335 and

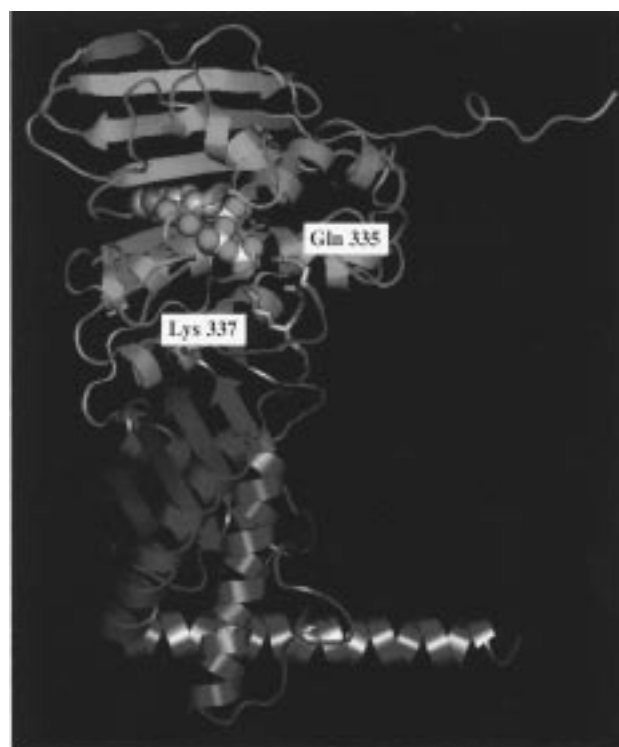
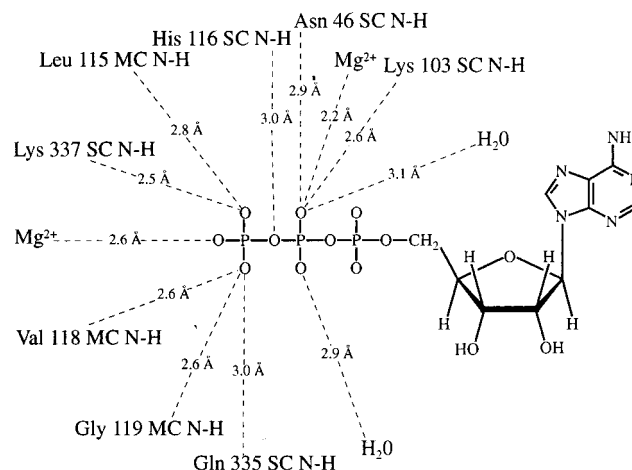


FIGURE 1: Interaction of amino acid residues in GyrB with ATP. (Top) Interaction of amino acid residues in GyrB with the nucleotide-binding site showing hydrogen bonding to the β - and γ -phosphate oxygens, derived from the X-ray crystallography model (8). MC, main chain; SC, side chain. (Bottom) X-ray crystal structure of the GyrB43 in complex with ADPNP. Subdomain 1 (residues 2–220) is indicated in purple, subdomain 2 (residues 221–393) is indicated in green. ADPNP is shown within subdomain 1. Gln335 and Lys337, including their side chains, are on a loop of subdomain 2 which reaches up to the nucleotide-binding site. The structure is a dimer, but here a monomer is shown for clarity.

Lys337. It has been proposed that these residues may provide a mechanism for signaling the hydrolysis of ATP to the rest of GyrB, i.e., initiating conformational changes following ATP hydrolysis (8). In this paper, we use site-directed mutagenesis to investigate the role of these residues in ATP hydrolysis by DNA gyrase.

EXPERIMENTAL PROCEDURES

Site-Directed Mutagenesis. Site-directed mutagenesis was carried out on the gene encoding the 43 kDa N-terminal GyrB fragment in plasmid pAJ1 (12) using a two-step

overlap-extension PCR method (26) to create mutations of Gln335 to Asn, Gln335 to Ala, Lys337 to Gln, and Lys337 to Ala, as described previously by Jackson and Maxwell (23). Site-directed mutagenesis of the gene encoding GyrB in plasmid pAG111 (27) was carried out using QuikChange (Stratagene). Briefly, two complementary oligonucleotides bearing the required mutation were incorporated into plasmid pAG111 during temperature cycling using *Pfu* polymerase. After digestion with *DpnI*, which removes the parental methylated template, the nicked plasmids were transformed into high competency *E. coli* XL1-Blue (Stratagene). The DNA sequence was confirmed by automated sequencing using a *Taq* DyeDeoxy Terminator Sequencing kit (Applied Biosystems). For GyrB43 mutants, the sequence of the insert DNA was confirmed. For GyrB mutants, the full gene was sequenced.

Enzymes and DNA. The DNA gyrase A and B proteins and the GyrB43 proteins were prepared as described previously for wild-type and soluble mutants (12, 27). Where proteins were insoluble and thought to be in inclusion bodies, cell extract pellets were washed four times in 1% Triton-X100 and repelleted. The pellet was then subjected to successive washes of 2, 4, 6, and 8 M urea in enzyme buffer (50 mM Tris-HCl, pH 7.5, 100 mM KCl, 2 mM DTT, 1 mM EDTA, and 10% w/v glycerol) and the pellet collected by centrifugation after each wash. The soluble fraction from each wash was examined by SDS-PAGE. Proteins in inclusion bodies were found in the 6 and 8 M urea washes. These proteins were dialyzed extensively against enzyme buffer. Negatively supercoiled and relaxed forms of plasmid pBR322 were prepared as described previously (28). Linear pBR322 was prepared by digestion of the supercoiled form by *EcoRI*.

Enzyme Assays. DNA supercoiling and relaxation assays were carried out as described previously (5). One unit of supercoiling activity was defined as the amount of enzyme required to convert 50% of relaxed pBR322 substrate to supercoiled product. Activities were expressed in terms of units per milligram of gyrase protein. Quinolone-induced cleavage assays were carried out using relaxed or linear pBR322, as described by Critchlow and Maxwell (29). ATPase assays were performed using the PK/LDH (pyruvate kinase/lactate dehydrogenase) linked assay as described by Ali et al. (12). ATPase activities of GyrB were measured in the presence of excess wild-type GyrA and linear pBR322 (greater than 1 gyrase/200 base pairs of DNA). The ATPase data for GyrB43 were fitted to a steady-state rate equation (12) using MacCurveFit 1.3 (Kevin Raner Software, Mt. Waverley, Australia). Nucleotide- and drug-binding assays were performed using Sephadex G50 Nick Spin columns (Pharmacia) based on the method of Tamura et al. (30). In nucleotide-binding experiments, [α - 32 P]ADPNP (29.6 TBq/mmol; ICN) or [2,8- 3 H]ADPNP (1.1 TBq/mmol; ICN) were used as described previously (22). The data were fitted to first-order exponentials [$A = A_{\infty}(1 - e^{-kt})$] to give a pseudo-first-order rate constant (k) and amplitude of ADPNP binding (A_{∞}). Second-order rate constants were obtained by dividing k by the ADPNP concentration to give values for k_{on} . Dissociation rates were determined by incubating 10 μ M enzyme with 350 μ M [2,8- 3 H]ADPNP using the procedure described previously (22). The data were fitted to a first-order exponential decay equation to give the dissociation rate

constant (k_{off}). Drug-binding assays, as described by Gormley et al. (19), were carried out using [3 H]dihydronovobiocin (2.07 TBq/mmol; Amersham).

Other Methods. Protein cross-linking using dimethyl suberimidate was performed as described previously (22) in a method adapted from Thomas (31). For experiments using ATP, 10 μ M protein was incubated minus or plus 1 mM ATP for 10 min at 25 °C, then cross-linker was added as previously described. Protein cross-linking in the presence of a range of coumermycin concentrations from 0 to 20 μ M was carried out as described previously (19). Novobiocin-Sepharose columns were made as described by Staudenbauer and Orr (20) and protein samples were applied and eluted as described by Gilbert and Maxwell (32). Temperature-sensitive complementation experiments using mutants of GyrB were carried out with strain N4177 [*strA galK gyrB221 (cou^R) gyrB203 (ts)*] (33). N4177 containing pAG111 encoding wild-type GyrB or the mutant variants of this plasmid were grown on Luria-Bertani agar plates containing 50 μ g mL $^{-1}$ ampicillin in the absence or presence of IPTG at a range of concentrations up to 50 μ M. Growth at 30 and 42 °C was determined. Circular dichroism analysis to verify the folding of wild-type and mutant proteins was carried out by Professor N. C. Price and Dr. S. Kelly (University of Stirling) to give CD spectra in the near and far UV. Amino acid sequence alignments were carried out using the University of Wisconsin Genetic Computer Group program PILEUP.

RESULTS

Proposed Role for Gln335 and Lys337. Close examination of the X-ray crystal structure of the 43 kDa N-terminal domain of GyrB around the nucleotide-binding site has allowed us to identify amino acid residues which are likely to be involved in ATP binding and hydrolysis. Figure 1, top panel, shows hydrogen-bonding contacts to the β - and γ -phosphate oxygens. Most of the amino acids contacting the nucleotide lie within subdomain 1 (residues 2–220). However, there are two residues which are within hydrogen-bonding distance of the γ -phosphate oxygens and are within subdomain 2 (residues 221–393). These are Gln335 and Lys337, which lie on a loop reaching up to the nucleotide-binding site, at distances of 3.0 and 2.5 Å, respectively (Figure 1, bottom panel). When subdomain 1 was expressed (a 24 kDa protein), it was shown that this fragment is unable to hydrolyze ATP and is unable to bind ATP, ADPNP, or ADP and binds ADP plus phosphate only very weakly (32). These results point to the importance of amino acid residues in subdomain 2 for nucleotide interaction; attention is focused on Gln335 and Lys337.

Further evidence for the importance of these two residues comes from amino acid sequence alignments. Comparison of *E. coli* GyrB with other bacterial GyrBs, as well as bacterial ParEs, bacteriophage T4 gp 39, and eukaryotic type II topoisomerases, indicate that these residues are totally conserved, and lie in a region of high conservation (34). Previously, it has been proposed that Gln335 and Lys337 may provide a mechanism for signaling hydrolysis of ATP to the rest of GyrB, i.e., initiating conformational changes following ATP hydrolysis (8). Other possibilities are that they are involved in the binding of nucleoside triphosphate

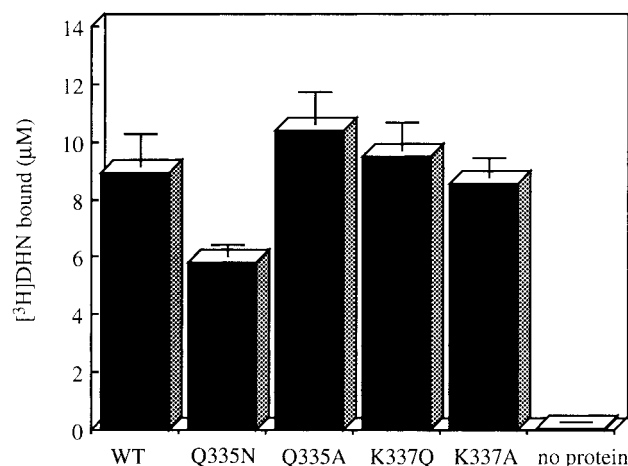


FIGURE 2: Binding of [^3H]dihydronovobiocin (DHN) (19) to wild-type and mutant 43 kDa proteins. Protein ($10\ \mu\text{M}$) was incubated with $50\ \mu\text{M}$ [^3H]DHN for 4 h at $25\ ^\circ\text{C}$. Protein-bound drug and unbound drug were separated using spin columns. Total bound drug was estimated by scintillation counting.

or that they play a role in transition-state stabilization during the hydrolysis reaction. To test these proposals, we have used site-directed mutagenesis to create mutations of Gln335 to asparagine and alanine and Lys337 to glutamine and alanine in the N-terminal domain of GyrB (GyrB43).

Production of Mutant 43 kDa Proteins. The level of expression of the mutated 43 kDa proteins was similar to that of the wild-type protein (data not shown). GyrB43^{Q335A} and GyrB43^{K337Q} were mainly in the soluble fraction of the cell extract and were purified conventionally (12). GyrB43^{Q335N} and GyrB43^{K337A} were mainly in the insoluble fraction and were purified from inclusion bodies.

Coumarin Drug Binding. Coumarin drug binding was investigated for wild-type and mutant proteins. We know that the novobiocin drug-binding site is in the N-terminal domain of GyrB, partially overlapping with the ATP-binding site (17), but does not involve Gln335 or Lys337; therefore, we would predict coumarin drug binding to be unchanged for the mutants, if they are correctly folded. First, binding of purified protein to a novobiocin-Sepharose column was investigated. Wild-type GyrB43 bound tightly to novobiocin and was only eluted with 6 M urea. The four mutant proteins also bound tightly to the column, eluting at 4–6 M urea (data not shown). Second, dihydronovobiocin binding (DHN) was investigated using radiolabeled drug and rapid gel filtration (19). GyrB43 protein ($10\ \mu\text{M}$) was incubated with $50\ \mu\text{M}$ drug for 4 h at $25\ ^\circ\text{C}$. Figure 2 shows DHN binding for wild-type and mutant proteins. Stoichiometries for wild-type GyrB43, GyrB43^{Q335A}, and GyrB43^{K337Q} are close to 1:1 as expected (12, 19, 22), slightly reduced for GyrB43^{K337A}, and only ~ 0.6 for GyrB43^{Q335N}, possibly suggesting that coumarin drug binding has been reduced due to misfolding of a proportion of the Q335N mutant. Also, protein cross-linking in the presence of a range of concentrations of coumermycin showed dimerization for each mutant as was previously obtained with the wild-type enzyme [data not shown (19)].

CD Spectroscopy. The wild-type GyrB43 and GyrB43^{Q335A} and GyrB43^{K337Q} and GyrB43^{K337A} proteins were analyzed by CD spectroscopy (carried out by Prof. N. C. Price and Dr. S. Kelly, University of Stirling). Evidence from the far-

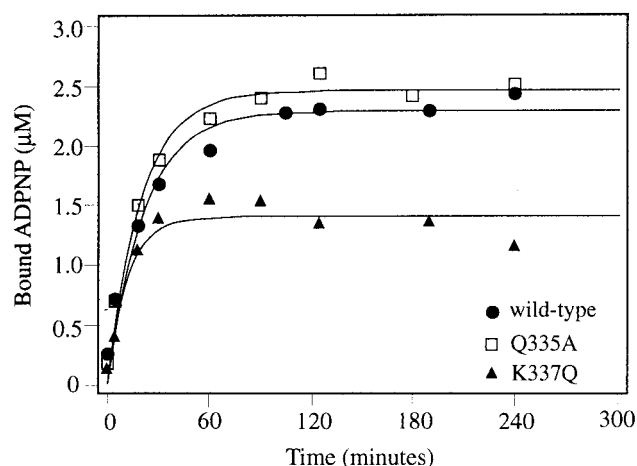


FIGURE 3: Binding of [$2,8\text{-}^3\text{H}$]ADPNP to wild-type and mutant 43 kDa GyrB. Binding experiments were at $10\ \mu\text{M}$ protein in the presence of $300\ \mu\text{M}$ [$2,8\text{-}^3\text{H}$]ADPNP. The amount of nucleotide bound to protein was determined at the times indicated by spin columns and scintillation counting. Data were fitted to first-order exponential equations using MacCurveFit.

UV spectra indicate that the secondary structure of wild-type, Q335A, and K337Q proteins are very similar; these mutations have not significantly altered the secondary structure. The near-UV spectra confirm that the tertiary structures of Q335A and K337Q are also very similar to the wild-type enzyme (data not shown). Far-UV CD spectra of K337A show a weaker signal (60%) than wild-type, and this is interpreted as only a proportion of the protein being folded. Also, in the near-UV spectra, there is a difference in the Tyr and Phe regions, indicating that the tertiary structure is likely to be different in K337A.

On the basis of drug-binding assays and CD analysis, Q335A and K337Q appear to be folded correctly. These two mutants were analyzed with respect to nucleotide binding and ATP hydrolysis. No further assays were carried out with Q335N and K337A due to their possible misfolding indicated by coumarin drug binding and CD analysis.

ADPNP Binding. The kinetics of ADPNP binding to GyrB43 was measured using rapid gel-filtration (spin columns) (Figure 3). In these experiments, $10\ \mu\text{M}$ 43 kDa protein was incubated with $300\ \mu\text{M}$ ADPNP. Under these conditions, full binding was previously observed within 60 min (22). Data were fitted to first-order exponentials to give pseudo-first-order rate constants and amplitudes for ADPNP binding. Second-order rate constants were obtained by dividing the pseudo-first-order rate constants by the ADPNP concentration. The amplitudes, indicating the total amount of bound ADPNP, were very similar for wild-type and Q335A. Second-order rate constants for ADPNP binding were also very similar for wild-type GyrB43 and Q335A: 2.61 and $2.83\ \text{M}^{-1}\text{s}^{-1}$ respectively. The second-order rate constant for K337Q was $4.8\ \text{M}^{-1}\text{s}^{-1}$ and the maximum amplitude of binding of K337Q was reduced to $\sim 60\%$ of wild-type. These data indicate that ADPNP binding is essentially unchanged between wild-type and Q335A, but that nucleotide binding to K337Q is impaired. We also observed a small loss in binding activity after 3–4 h at $25\ ^\circ\text{C}$ with GyrB43^{K337Q}. Although the coumarin drug binding and CD analysis for this mutant indicated that this protein is folded correctly, there may be some loss in stability compared to the wild-type enzyme over several hours.

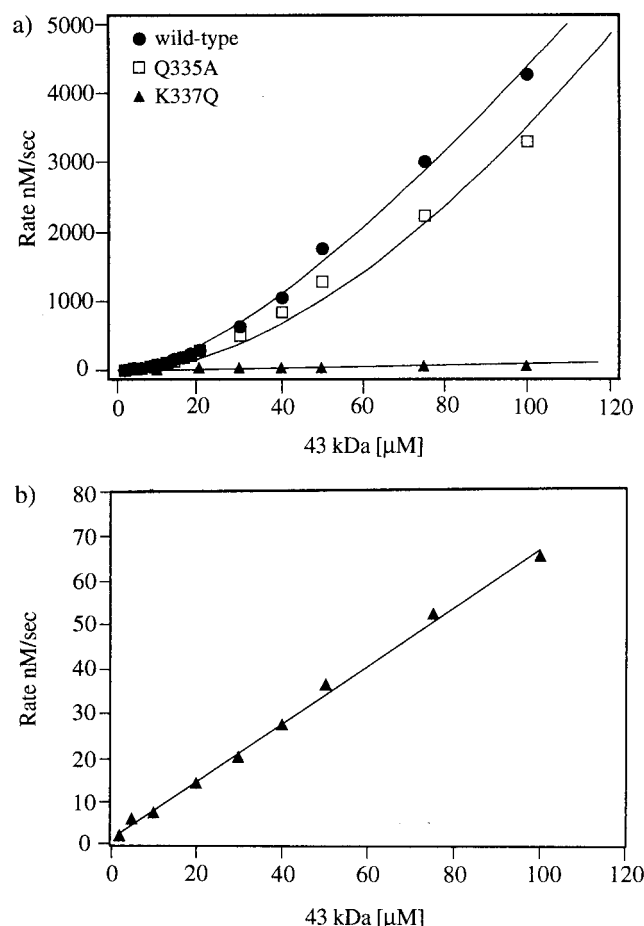


FIGURE 4: ATPase activities of wild-type GyrB43, GyrB43^{Q335A}, and GyrB43^{K337Q} as a function of enzyme concentration. Rates are initial velocities measured using the PK/LDH linked enzyme assay. The substrate concentration was 2 mM. Rates are novobiocin sensitive. (a) ATPase activities of wild-type GyrB43, GyrB43^{Q335A}, and GyrB43^{K337Q} are shown. Wild-type and Q335A are not linearly dependent on enzyme concentration over the range 2–100 μM. These data are fitted to the steady-state rate equation (12) for ATP hydrolysis by 43 kDa GyrB. (b) ATPase data for GyrB43^{K337Q} from panel 4a show a linear dependence on enzyme concentration.

The spin-column method was also used to determine the rate of dissociation of ADPNP from wild-type and Q335A enzymes. Protein (10 μM) was incubated with 350 μM ADPNP for 2 h. Unbound nucleotide was removed on a spin column. The eluted protein–ADPNP complex was diluted 10-fold and incubated with 50-fold excess of cold ADPNP. At time points up to 30 h, bound ADPNP was measured (data not shown). The dissociation rates were found to be slow, $\sim 10^{-6} \text{ s}^{-1}$, as reported previously (22), for both wild-type and GyrB43^{Q335A}. Dissociation experiments for the GyrB43^{K337Q} protein proved to be problematic as the protein appeared to lose binding activity over the long period of time required in these experiments, as mentioned above.

ATP Hydrolysis by Wild-Type and Mutant Proteins. ATP hydrolysis by wild-type GyrB43 has been studied previously (12). The enzyme displays non-Michaelis–Menten kinetics, with a greater than first-order dependence of rate on enzyme concentration. At constant enzyme concentrations there is an apparent hyperbolic dependence of rate on substrate concentration. A model has been proposed for the ATPase cycle (ref 12; see Figure 7).

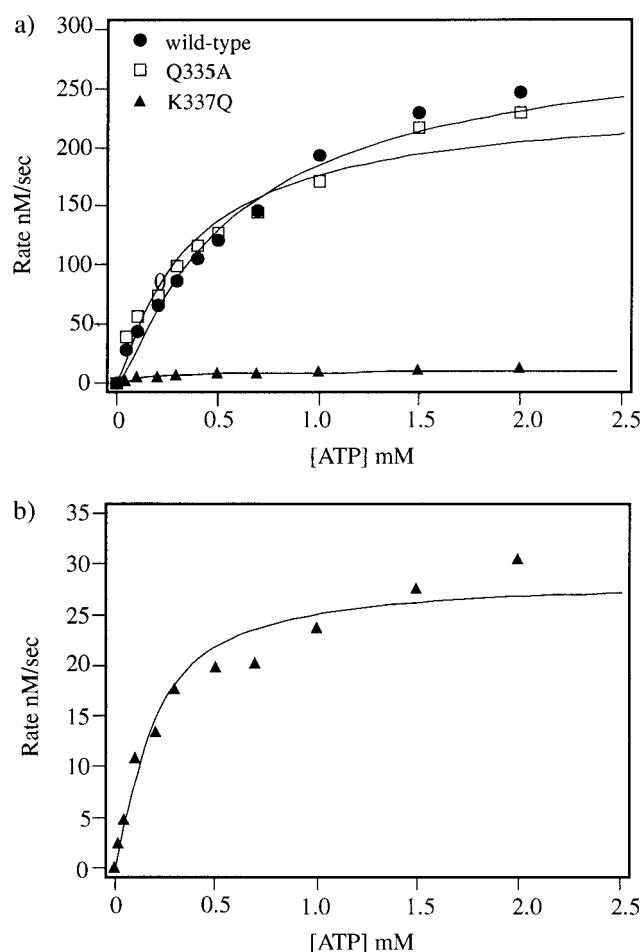


FIGURE 5: (a) ATPase activity of 20 μM wild-type GyrB43, GyrB43^{Q335A}, and 50 μM GyrB43^{K337Q} as a function of ATP concentration. Data were fitted to the steady-state rate equation for ATP hydrolysis by 43 kDa GyrB (12). (b) Data for the mutant GyrB43^{K337Q} from panel a were also fitted to a rectangular hyperbola.

ATP hydrolysis by wild-type GyrB43, GyrB43^{Q335A}, and GyrB43^{K337Q} was investigated as a function of enzyme concentration (Figure 4a). Assays were carried out at protein concentrations in the range 2–100 μM using 2 mM ATP. The wild-type enzyme shows a nonlinear dependence of the rate on enzyme concentration as previously reported (12). At a concentration of 40 μM, the turnover number for wild-type enzyme was 0.026 s^{-1} . ATP hydrolysis by Q335A also demonstrated this nonlinear dependence of rate on enzyme concentration, and the turnover number was 0.021 s^{-1} at 40 μM. These data were fitted to the steady-state rate equation previously described (12). As shown in Figure 4a, ATP turnover for K337Q is much lower than for wild-type enzyme. At 40 μM, turnover by K337Q was 0.00068 s^{-1} ; a 40-fold reduction in the rate compared to the wild-type enzyme. Interestingly, the rate of ATP hydrolysis by K337Q is apparently linear with respect to enzyme concentration. Figure 4b shows that these data for K337Q can be fitted to a straight line. This shows that there is a change in the rate-limiting step of the reaction cycle with this mutant, i.e., it is no longer dimerization. We observed no decrease in the ATPase rate during the assays, therefore GyrB43^{K337Q} appears to be stable at 25 °C over the time course of the assay (typically 30–60 min).

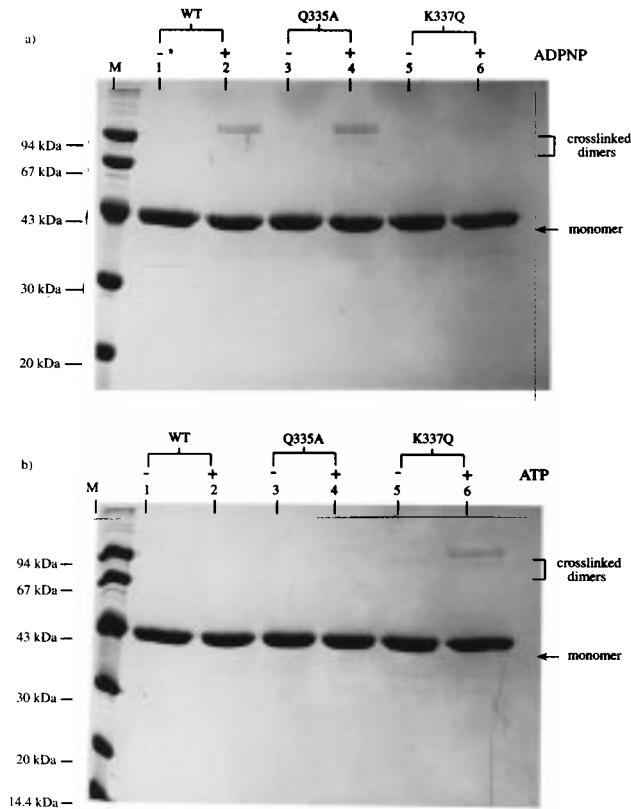


FIGURE 6: (a) Cross-linking of the wild-type and mutant 43 kDa proteins in the presence of ADPNP with dimethyl suberimidate (DMS). Protein (10 μ M) was incubated for 1 h at 25 $^{\circ}$ C plus or minus 1 mM ADPNP. DMS (4 mg mL $^{-1}$) was added at 0 and 2 h. Samples were analyzed by SDS-PAGE after 4 h. (b) Cross-linking of the wild-type and mutant 43 kDa proteins in the presence of ATP with (DMS). Protein (10 μ M) was incubated for 10 min at 25 $^{\circ}$ C plus or minus 1 mM ATP. DMS (4 mg mL $^{-1}$) was added at 0 and 2 h. Samples were analyzed by SDS-PAGE after 4 h.

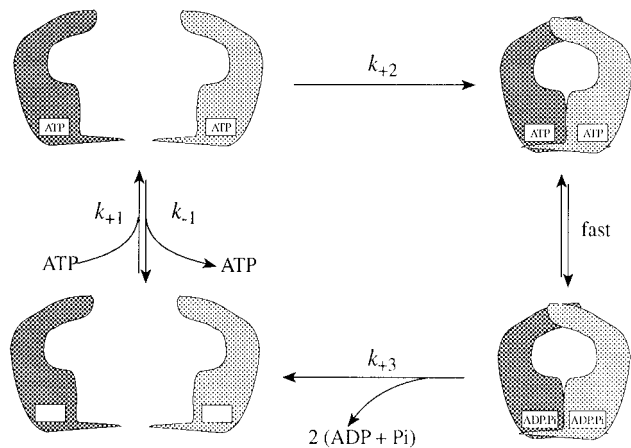


FIGURE 7: Model for the ATPase cycle of GyrB43, redrawn from Ali et al. (12).

The rate of ATP hydrolysis as a function of substrate (ATP) concentration has also been investigated. For wild-type GyrB43 and GyrB43^{Q335A} at 20 μ M and GyrB43^{K337Q} at 50 μ M, initial rates of hydrolysis at a range of ATP concentrations from 0.05 to 2 mM were measured. These data are shown in Figure 5a. Data were fitted to the steady-state rate equation and rate constants were obtained (see Discussion; Table 1). These data K337Q versus ATP concentration were also fitted to a rectangular hyperbola (Figure

Table 1: Comparison of the Kinetic Parameters of Wild-Type GyrB43, GyrB43^{Q335A}, and GyrB43^{K337Q}

kinetic parameters ^a	values from Ali et al. (12)	wild-type	Q335A	K337Q
k_{+1}	121 M $^{-1}$ s $^{-1}$	124 M $^{-1}$ s $^{-1}$	122 M $^{-1}$ s $^{-1}$	121 M $^{-1}$ s $^{-1}$
k_{-1}	0.0083 s $^{-1}$	0.0156 s $^{-1}$	0.0101 s $^{-1}$	0.135 s $^{-1}$
k_{+2}	293 M $^{-1}$ s $^{-1}$	333 M $^{-1}$ s $^{-1}$	295 M $^{-1}$ s $^{-1}$	292 M $^{-1}$ s $^{-1}$
k_{+3}	1.26 s $^{-1}$	2.03 s $^{-1}$	1.76 s $^{-1}$	0.00075 s $^{-1}$

kinetic parameters ^b	K337Q
V_{\max}	3.5×10^{-8} M s $^{-1}$
K_M	3.5×10^{-4} M
k_{cat}	0.000 70 s $^{-1}$

^a Kinetic parameters were derived by fitting ATPase rates to the steady-state rate equation (12) using MacCurveFit (version 1.3). ^b Data for GyrB43^{K337Q} were also fitted to the Michaelis-Menten equation.

5b). Values for K_M and V_{\max} are indicated in Table 1 (see Discussion).

Cross-Linking of Protein-Nucleotide Complexes. X-ray crystallography has shown that GyrB43 is a dimer in the presence of ADPNP, and there is evidence from gel filtration and equilibrium sedimentation that also support this idea (12). Protein cross-linking studies also show that dimers occur in the presence of ADPNP (22). Dimethyl suberimidate is a widely used protein cross-linking agent (35), which can react with primary amino groups (e.g., lysines) in proteins. When 10 μ M wild-type GyrB43 protein was incubated with dimethyl suberimidate, there were no cross-linked products (Figure 6a, lane 1). However, in the presence of ADPNP (1 mM), cross-linked products can be formed (Figure 6a, lane 2) which have molecular masses that are consistent with dimers of the 43 kDa. Mutants GyrB43^{Q335A} and GyrB43^{K337Q} were tested under the same conditions for ADPNP-induced dimer formation by cross-linking. These results are shown in Figure 6a, lanes 4 and 6. Both mutants form the cross-linked dimer in the presence of ADPNP and not in its absence. The dimer band with Q335A is of equal intensity to that of wild-type. The dimer of K337Q in the presence of ADPNP is weaker than for wild-type. As previously shown from spin column experiments, ADPNP binding to this mutant is reduced to about 60%, consistent with a reduced cross-linked dimer band with K337Q.

Protein cross-linking in the presence of ATP was compared for wild-type GyrB43, GyrB43^{Q335A}, and GyrB43^{K337Q}. In these experiments, 10 μ M protein was incubated with 1 mM ATP for 10 min, then the cross-linker was added. These results are shown in Figure 6b. Wild-type GyrB43 and Q335A show identical results, i.e., no dimers are formed, consistent with earlier findings (George Orphanides, personal communication). However, with K337Q, there is a distinct increase in the intensity of the dimer band in the presence of ATP. This implies that, for this mutant, the nucleotide-bound dimer is stabilized.

Mutations in GyrB. Mutations of Gln335 to asparagine and alanine and Lys337 to glutamine and alanine were also made in full-length GyrB. GyrB^{Q335A} was purified in the same way as conventional GyrB. It was noted that *E. coli* XL1-Blue cells containing the plasmid carrying GyrB^{K337Q} grew more slowly than those containing wild-type GyrB. Also, GyrB^{K337Q} was partially in the soluble fraction and partially in the insoluble fraction of the cell extract and was

Table 2: Comparison of the Properties of Wild-Type GyrB, GyrB^{Q335A}, and GyrB^{K337Q}

property ^a	WT GyrB	GyrB ^{Q335A}	GyrB ^{K337Q} ^b
expression	soluble	soluble	partially soluble/partially in inclusion bodies
DNA supercoiling	100%	100%	<1%
DNA relaxation	100%	100%	100%
quinolone-induced DNA cleavage	100%	100%	80–90%
ATPase (s ⁻¹)			
–DNA	0.247	0.100	<0.02
+DNA	0.431	0.104	<0.02
complementation of ts N4177	+	+	–

^a DNA supercoiling, relaxation, cleavage, and ATPase activities were measured in the presence of wild-type GyrA. ^b Data shown are for GyrB^{K337Q} purified from the insoluble fraction of the cell extract, however assays were also carried out with GyrB^{K337Q} from the soluble fraction, and very similar results were obtained.

purified and assayed from both fractions. Assay results were very similar with GyrB^{K337Q} from either source.

On the basis of the results with GyrB43, we would predict that GyrB^{Q335A} should behave like wild-type enzyme, and neither the ATP-dependent or ATP-independent reactions should be affected. With GyrB^{K337Q}, the ATP-independent reactions are likely to be unaffected, as long as this mutation has not caused any changes in the structure of the enzyme; however, ATP-dependent reactions (ATP hydrolysis and DNA supercoiling) are likely to be impaired.

In the absence of ATP, DNA gyrase can relax supercoiled DNA. We have compared the relaxation activities of wild-type GyrB, GyrB^{Q335A}, and GyrB^{K337Q} in the presence of excess GyrA. The activities are very similar (Table 2). Quinolone-induced DNA cleavage in the absence of ATP was also found to be similar for all three proteins (Table 2), i.e., gyrase complexes which contain the mutant GyrBs are as active as wild-type GyrB with respect to cleavage. These experiments support the idea that the mutants are folded and are able to interact with GyrA, in the A₂B₂ complex, in the normal way. DNA gyrase introduces negative supercoils into closed-circular DNA in the presence of ATP. DNA supercoiling activities of wild-type GyrB, GyrB^{Q335A}, and GyrB^{K337Q} were compared. Wild-type and Q335A both demonstrate supercoiling activities of ~10⁵ units mg⁻¹, consistent with the results obtained previously, showing that ATP-dependent DNA supercoiling has been unaffected by mutation of Gln335. No difference between the supercoiling activity of wild-type GyrB and GyrB^{Q335A} was detectable over a 10-fold range of enzyme concentrations or over time courses of up to 2 h (data not shown).

There was no detectable supercoiling by K337Q; the activity was less than 1% of wild-type. It is clear that supercoiling activity has been grossly impaired by mutation of K337Q. It is beyond the limits of detection of the supercoiling assay to determine a precise activity between 0 and 1%, but since we know with GyrB43^{K337Q} we observed a large reduction in ATP turnover (40-fold at an enzyme concentration of 40 μM), then the inability of this mutant protein to supercoil DNA is not unexpected and is likely to be a result of its impaired ATPase activity. It is possible that at high concentrations of GyrB^{K337Q} some supercoiling may be observed.

Wild-type GyrB has intrinsic ATPase activity which is stimulated by the addition of GyrA and DNA (21). ATPase activities were measured for wild-type and mutant GyrBs and the results are shown in Table 2. There is some

stimulation of ATP turnover by GyrA and DNA for wild-type enzyme but this is much lower than previously reported values (21). By comparison, GyrB^{Q335A} shows less than 50% of the intrinsic activity of wild-type, and no stimulation upon the addition of GyrA and DNA. GyrB^{K337Q} ATPase rates were more than 10-fold lower than wild-type rates even in the presence of GyrA and DNA.

Temperature-sensitive complementation experiments were carried out in strain N4177 [*strA galK gyrB221 (cou^R) gyrB203 (ts)*] (33). This strain grows at 30 °C but not at 42 °C. Plasmids bearing GyrB with the mutations Q335N, Q335A, K337Q, and K337A were transformed into N4177 cells, and growth at 30 °C and 42 °C was tested and compared with growth of these cells bearing the wild-type plasmid. Results indicated that wild-type, Q335N-, and Q335A-bearing plasmids all complemented the ts phenotype and grew at 42 °C, however, K337Q- and K337A-bearing plasmids did not.

DISCUSSION

Since the cloning and purification of the N-terminal 43 kDa domain of GyrB, the crystal structure of this domain in complex with ADPNP has been solved to 2.5 Å resolution by X-ray crystallography (8). The biochemical properties of this domain have been well studied, with respect to nucleotide binding and coumarin drug binding (12, 19, 22). Also, ATP hydrolysis has been investigated and this has led to a steady-state rate equation for this reaction (12). As such, this is an ideal enzyme to study by site-directed mutagenesis. In this case, we examined the role of amino acid residues potentially involved in the ATPase reaction.

The mutations made in this study were Gln335 to Asn and Ala and Lys337 to Gln and Ala. All four GyrB43 mutants showed similar levels of overexpression to the wild-type enzyme. Mutants Q335N and K337A were largely in the insoluble fraction of the cell extract (i.e., in inclusion bodies) and, in order to purify them, were solubilized in 6–8 M urea. These enzymes were then refolded by extensive dialysis into enzyme buffer. Clearly, these mutants are behaving differently to the wild-type enzyme, which is expressed as a soluble protein, and this could be due to misfolding of the protein. A number of approaches were used to verify whether the mutants were folded correctly. First, coumarin drug binding was compared for wild-type and mutants. We would predict that coumarin drug binding should be unchanged for correctly folded enzymes, since we know that the drug-binding site partially overlaps with the

ATP-binding site (17), but does not involve Gln335 or Lys337. The results from binding to novobiocin affinity columns and protein cross-linking in the presence of coumermycin, suggest that coumarin drug binding is essentially like wild-type GyrB43 for the four mutants. Data from spin column experiments suggest that dihydronovobiocin drug binding is essentially 1:1 for wild-type, Q335A, and K337Q, but slightly reduced for K337A and reduced to about 60% for Q335N. This indicated that there maybe some misfolded or inactive protein in the Q335N sample.

CD analysis supported the idea that wild-type GyrB43, GyrB43^{Q335A}, and GyrB43^{K337Q} have comparable secondary and tertiary folds, with the far- and near-UV CD spectra for each being superimposable. The far-UV CD spectrum for GyrB43^{K337A} showed a weaker signal and this has been interpreted as only a proportion of the protein being folded correctly. Also, in the near UV there was a shift in the spectrum for K337A in the Tyr and Phe regions compared to the wild-type enzyme, suggesting that the tertiary fold of the protein is different to that of the wild-type enzyme.

It is clear from both the coumarin drug binding and CD spectroscopy that caution must be exercised when interpreting results from GyrB43^{Q335N} and GyrB43^{K337A}, since any differences from the wild-type enzyme may be due to misfolded, inactive enzyme rather than the specific amino acid change introduced. However, both GyrB43^{Q335A} and GyrB43^{K337Q} appear to be correctly folded. These two mutants were therefore used in subsequent assays where nucleotide binding and ATP hydrolysis were compared to wild-type enzyme, to determine the role if any, of residues Gln335 and Lys337, in the GyrB ATPase reaction.

Data for wild-type GyrB43 and GyrB43^{Q335A} enzymes show that ADPNP binding was unchanged with respect to both the apparent on-rate and amplitude of nucleotide binding, i.e., Gln335 does not appear to have a role in nucleotide binding (Figure 3). For GyrB43^{K337Q}, however, the amplitude of ADPNP binding was reduced to about 60% of that for wild-type; the on-rate was somewhat faster. This suggests that the amino acid Lys337 may have a role in nucleotide binding. There are other residues which have been shown to be essential in binding of ADPNP, for example, Lys103, which forms a salt bridge with the β -phosphate of the nucleotide triphosphate. When this residue was mutated to threonine, glutamate, or isoleucine, ADPNP binding was abolished (25). By contrast, mutation of Lys337 has reduced ADPNP binding, but not abolished it. Therefore, Lys337 does not appear to be essential for binding of ADPNP, but it may be that replacing Lys with Gln has caused a perturbation of the nucleotide-binding site, changing the interaction of the protein with nucleoside triphosphate. However, this reduction in ADPNP binding for the Lys337 to Gln mutant is not sufficient to account for the reduced ATPase rates observed.

Protein cross-linking experiments provide evidence for a stabilized nucleotide-bound dimer complex in the case of GyrB43^{K337Q}. The results of cross-linking in the presence of ADPNP show again that there is no observable difference between wild-type GyrB43 and GyrB43^{Q335A}. ADPNP binding and ADPNP-promoted dimerization appear to be unchanged in this mutant. With K337Q in the presence of ADPNP, however, there was a decrease in intensity of the dimer band, and this is consistent with the reduction in

ADPNP binding observed from spin column experiments. In the presence of ATP, GyrB43^{Q335A} produced no dimer band as observed with the wild-type enzyme. However, there was an observable dimer band for the K337Q protein in the presence of ATP (Figure 6b, lane 6). These observations can be rationalized by considering the proposed scheme for ATP hydrolysis in Figure 7. ATP binds to GyrB43, two monomers come together, ATP is rapidly hydrolyzed, products dissociate, and the monomers reform. When ATP is being turned over, the lifetime of the dimer is short (for most of the cycle the enzyme is a monomer); therefore, there are virtually no cross-links formed to give dimers in the presence of ATP. The result with the wild-type enzyme and ADPNP can be rationalized since ADPNP is a nonhydrolyzable ATP analogue and ADPNP stabilizes the dimer so cross-links can be formed. It seems that, with ATP and the GyrB43^{K337Q} protein, the dimer complex is also being stabilized in comparison with the wild-type enzyme in the presence of ATP. This could be accounted for if ATP hydrolysis has been slowed in this mutant such that ATP remains bound for a longer time, or the products of ATP hydrolysis (ADP and phosphate) do not dissociate as rapidly. This suggests that it may be the catalytic step which is altered in the K337Q mutant.

The ATPase reaction of wild-type GyrB43 has been studied in detail (12), and the enzyme has been shown to display non-Michaelis–Menten kinetics with a greater than first-order dependence of rate on enzyme concentration. This is consistent with the rate-limiting step being oligomerization, and there are several lines of evidence which show that the GyrB43 enzyme is active as a dimer. A model for the ATPase cycle has been proposed (Figure 7) and a steady-state rate equation based on this model has been derived (12).

The ATPase reaction for GyrB43^{Q335A} and GyrB43^{K337Q} has been studied as a function of both enzyme and ATP concentrations (Figures 4a and 5a). To a good approximation, Q335A behaves like wild-type and the ATPase data can be accommodated by the scheme shown in Figure 7 and fitted to the steady-state rate equation derived by Ali et al. (12). The rate constants determined are shown in Table 1. Although the data in Figures 4a and 5a are insufficient to uniquely define these rate constants, it is clear that Q335A and the wild-type enzyme are very similar with respect to the hydrolysis of ATP.

When the data for GyrB43^{K337Q} are fitted to the steady-state rate equation from Ali et al. (12), it is clear that the rate of hydrolysis (k_{+3}) has to be reduced dramatically ($> 10^3$) to accommodate these data (Table 1). Although the other rate constants are similar to wild-type, except for k_{-1} , there are insufficient data to draw any further conclusions. In the case of k_{-1} , the ~ 10 -fold increase is consistent with the apparent loss of stability of the complex with ADPNP (Figure 3). The data for K337Q were also fitted to the Michaelis–Menten equation (Figure 5b), and values for K_M and V_{max} were obtained (Table 1). The apparent linear dependence of rate on enzyme concentration suggests that this may be appropriate for this mutant. Interestingly, the value for k_{cat} of 0.0007 s^{-1} obtained from the Michaelis–Menten fit is very close to the rate constant k_{+3} (0.00075 s^{-1}) obtained from the steady-state equation fit. This strongly reinforces the idea that it is the turnover number which has been greatly reduced by mutation of Lys337 to Gln.

The results with the mutations in full-length GyrB corroborate the data obtained with the mutations in the 43 kDa N-terminal domain. Complementation experiments of the *E. coli* temperature-sensitive strain N4177 support the idea that Gln335 does not appear to be an essential residue for the functional enzyme in vivo. GyrB containing Q335N or Q335A both rescued the temperature-sensitive phenotype of N4177 at 42 °C. On the other hand, GyrB-containing mutations at amino acid residue 337 showed no complementation at 42 °C. This suggests that these mutant proteins are unable to function well enough in vivo to support cell growth, and this is likely to be due to its deficiency in ATP hydrolysis. Similar temperature-sensitive complementation experiments were used with the active-site residue mutants of GyrB (23). When Glu42 was mutated to Gln and Ala, neither showed complementation of the temperature-sensitive phenotype, supporting the idea for the importance of this residue.

GyrB^{Q335A} behaved essentially like the wild-type enzyme, in all the ways characterized. For DNA cleavage and DNA relaxation, which do not require ATP, activities for GyrB^{Q335A} were indistinguishable from those of the wild-type enzyme. We would expect the ATP-independent functions of GyrB to be unaffected by this mutation, unless the enzyme is misfolded, and these results support the idea that this mutant is likely to be folded correctly and it is able to interact with GyrA and DNA. Also, from the results obtained for GyrB43^{Q335A}, we would predict that the ATP-dependent reaction of GyrB^{Q335A} would be unaffected. This is confirmed by the DNA-supercoiling activity which was also indistinguishable from that of wild-type. However, ATP hydrolysis was lower than for the wild-type enzyme, and there was little or no stimulation of ATPase by the addition of GyrA and DNA. The significance of this result is not clear. It has been observed that there is variation between wild-type GyrB activities, and in particular, there is a large variation in the level of stimulation observed when GyrA and DNA are added (21, 22, 36). Therefore, it may be possible to explain the reduced ATPase activity of Q335A by being at the lower end of the activity range observed for GyrB preparations. The results of GyrB^{Q335A} ATPase assays do not rule out the possibility that ATP hydrolysis has been affected in a minor way with this mutant. In the A₂B₂ complex, where the dimerization is not thought to be rate-limiting, then a small change in the ATP hydrolysis rate might be detectable, unlike with GyrB43 where dimerization is slow and so conceals small decreases in the hydrolysis rate. However, a change in hydrolysis by GyrB^{Q335A} is not substantiated by the DNA-supercoiling data. It seems likely that the reduction in GyrB^{Q335A} ATPase is not significant in this case.

The ATP-independent reactions of GyrB^{K337Q} were investigated and both quinolone-induced DNA cleavage and DNA relaxation activities were not significantly different to those of the wild-type enzyme. The same results were obtained whether GyrB^{K337Q} was purified from the soluble or insoluble fraction. These data support the idea that this enzyme is folded and is able to interact with GyrA, so that any differences in the ATP-dependent results can be attributed to the replacement of Lys337 with Gln rather than to misfolding of the enzyme. Both ATP-dependent reactions for this mutant are essentially abolished. No DNA super-

coiling was observed; the supercoiling activity was less than 1%. Clearly, the large impairment of ATP turnover in this Lys337 mutant results in the inability to drive DNA supercoiling. This is supported by ATPase data for K337Q, which show again that ATP turnover is greatly impaired, confirming that Lys337 must have an important role in ATP hydrolysis.

CONCLUSIONS

Despite the location and conservation of Gln335 in GyrB, site-directed mutagenesis has revealed no clear role for this residue in the ATP hydrolysis reaction. In GyrB43, ATP hydrolysis appears to be unaffected by the mutation to Ala, i.e., this mutation has not changed a rate-determining step in the reaction. Also, no evidence for the predicted role in initiating conformational changes following ATP hydrolysis could be established. If this were the case, we would expect the supercoiling activity to be changed in this mutant, but the results indicate that it was indistinguishable from wild-type GyrB. Replacement of Lys337 by Gln has a more drastic effect on ATP hydrolysis, resulting in an $\sim 10^3$ decrease in k_{cat} . Results of ADPNP-binding experiments with GyrB43^{K337Q} show that there is a small decrease in nucleotide binding; however, this on its own is insufficient to account for the large reduction in ATP turnover observed. The supercoiling and ATPase activities of GyrB^{K337Q} were undetectable despite the enzyme behaving like wild-type GyrB with respect to ATP-independent reactions. Clearly, Lys337 is an important residue in ATP hydrolysis by GyrB. The different effects of mutations at Gln335 and Lys337 can be rationalized by the differences in the nature of interactions between these two groups and the γ -phosphate of ATP. Glutamine makes a polar interaction while the interaction with lysine is ionic. Therefore, we would expect the loss of the interaction with lysine to have more profound effects, as indeed we observe. Although we cannot rule out more subtle effects from the loss of hydrogen bonding by Gln335, these experiments suggest that these would be insignificant compared to the effects from the loss of the interaction with Lys337. The effects of the Lys337 mutation on nucleotide binding are rather modest, whereas the effects on the k_{cat} of the ATPase of GyrB43 are drastic. Although these data do not rule out the possibility that Lys337 is also involved in a global conformational change, the results are consistent with its involvement in transition-state stabilization, and we propose that this is a major role of this residue.

ACKNOWLEDGMENT

We thank Janid Ali and Niall Gormley for helpful comments on the manuscript and Symon Erskine for help with the molecular graphics figures. We thank Professor N. C. Price and Dr. S. Kelly (University of Stirling) for carrying out the CD spectroscopy.

REFERENCES

1. Reece, R. J., and Maxwell, A. (1991) *CRC Crit. Rev. Biochem. Mol. Biol.* 26, 335–375.
2. Wigley, D. B. (1995) Structure and mechanism of DNA gyrase. In *Nucleic Acids and Molecular Biology* (Eckstein, F., and Lilley, D. M. J., Eds.) Vol. 9, pp 165–176, Springer-Verlag, Berlin, Heidelberg.

3. Sugino, A., Higgins, N. P., Brown, P. O., Peebles, C. L., and Cozzarelli, N. R. (1978) *Proc. Natl. Acad. Sci. U.S.A.* 75, 4838–4842.
4. Morais Cabral, J. H., Jackson, A. P., Smith, C. V., Shikotra, N., Maxwell, A., and Liddington, R. C. (1997) *Nature* 388, 903–906.
5. Reece, R. J., and Maxwell, A. (1989) *J. Biol. Chem.* 264, 19648–19653.
6. Reece, R. J., and Maxwell, A. (1991) *J. Biol. Chem.* 266, 3540–3546.
7. Reece, R. J., and Maxwell, A. (1991) *Nucleic Acids Res.* 19, 1399–1405.
8. Wigley, D. B., Davies, G. J., Dodson, E. J., Maxwell, A., and Dodson, G. (1991) *Nature* 351, 624–629.
9. Brown, P. O., Peebles, C. L., and Cozzarelli, N. R. (1979) *Proc. Natl. Acad. Sci. U.S.A.* 76, 6110–6114.
10. Gellert, M., Fisher, L. M., and O'Dea, M. H. (1979) *Proc. Natl. Acad. Sci. U.S.A.* 76, 6289–6293.
11. Adachi, T., Mizuuchi, M., Robinson, E. A., Appella, E., O'Dea, M. H., Gellert, M., and Mizuuchi, K. (1987) *Nucleic Acids Res.* 15, 771–784.
12. Ali, J. A., Jackson, A. P., Howells, A. J., and Maxwell, A. (1993) *Biochemistry* 32, 2717–2724.
13. Maxwell, A. (1997) *Trends Microbiol.* 5, 102–109.
14. Mizuuchi, K., O'Dea, M. H., and Gellert, M. (1978) *Proc. Natl. Acad. Sci. U.S.A.* 75, 5960–5963.
15. del Castillo, I., Vizán, J., Rodríguez-Sainz, M., and Moreno, F. (1991) *Proc. Natl. Acad. Sci. U.S.A.* 88, 8860–8864.
16. Contreras, A., and Maxwell, A. (1992) *Mol. Microbiol.* 6, 1617–1624.
17. Lewis, R. J., Singh, O. M. P., Smith, C. V., Skarynski, T., Maxwell, A., Wonacott, A. J., and Wigley, D. B. (1996) *EMBO J.* 15, 1412–1420.
18. Tsai, F. T. F., Singh, O. M. P., Skarzynski, T., Wonacott, A. J., Weston, S., Tucker, A., Pauptit, R. A., Breeze, A. L., Poyser, J. P., O'Brien, R., Ladbury, J. E., and Wigley, D. B. (1997) *Proteins: Struct., Funct., Eng.* 28, 41–52.
19. Gormley, N. A., Orphanides, G., Meyer, A., Cullis, P. M., and Maxwell, A. (1996) *Biochemistry* 35, 5083–5092.
20. Staudenbauer, W. L., and Orr, E. (1981) *Nucleic Acids Res.* 9, 3589–3603.
21. Maxwell, A., and Gellert, M. (1984) *J. Biol. Chem.* 259, 14472–14480.
22. Ali, J. A., Orphanides, G., and Maxwell, A. (1995) *Biochemistry* 34, 9801–9808.
23. Jackson, A. P., and Maxwell, A. (1993) *Proc. Natl. Acad. Sci. U.S.A.* 90, 11232–11236.
24. Tamura, J., and Gellert, M. (1990) *J. Biol. Chem.* 265, 21342–21349.
25. O'Dea, M. H., Tamura, J. K., and Gellert, M. (1996) *J. Biol. Chem.* 271, 9723–9729.
26. Ho, S. N., Hunt, H. D., Horton, R. M., Pullen, J. K., and Pease, L. R. (1989) *Gene* 77, 51–59.
27. Hallett, P., Grimshaw, A. J., Wigley, D. B., and Maxwell, A. (1990) *Gene* 93, 139–142.
28. Bates, A. D., and Maxwell, A. (1989) *EMBO J.* 8, 1861–1866.
29. Critchlow, S. E., and Maxwell, A. (1996) *Biochemistry* 35, 7387–7393.
30. Tamura, J. K., Bates, A. D., and Gellert, M. (1992) *J. Biol. Chem.* 267, 9214–9222.
31. Thomas, J. O. (1989) *Methods Enzymol.* 170, 549–571.
32. Gilbert, E. J., and Maxwell, A. (1994) *Mol. Microbiol.* 12, 365–373.
33. Menzel, R., and Gellert, M. (1983) *Cell* 34, 105–113.
34. Caron, P. R., and Wang, J. C. (1994) *Adv. Pharmacol.* 29B, 271–297.
35. Davies, G. E., and Stark, G. R. (1970) *Proc. Natl. Acad. Sci. U.S.A.* 66, 651–656.
36. Tingey, A. P., and Maxwell, A. (1996) *Nucleic Acids Res.* 24, 4868–4873.

BI9801309